*J. Plasma Physics* (2017), *vol.* 00, *part* 0, *pp.* 1–000.  
DOI: 10.1017/S0000000000000000 Printed in the United Kingdom

# Can we use the variations of the electrostatic potential along flux surfaces to control impurity transport in stellarators?

J. Arturo Alonso, Iván Calvo, José Manuel García-Regaña and José Luis Velasco

Laboratorio Nacional de Fusión, CIEMAT, Av. Complutense 40, 28040 Madrid, Spain

(Received 14 May 2017)

**Abstract.** Impurity transport is a subject of fundamental and practical interest in magnetically confined non-axisymmetric plasmas. An impurity transport mechanism that has received considerable recent attention is that due to the radial $E \times B$ advection of the variations of impurity density along the flux surfaces. We discuss some of the general characteristics of this mechanism that make it an interesting potential tool to counteract the accumulation of impurities in stellarators. The size and sign of this term is expected to depend on the collisionality regime as well as on the relative phase of the variations of the electrostatic potential and the impurity density along flux surfaces. Here we will discuss the size and parity under stellarator-symmetry transformations of the variations of electrostatic potential for low-ion-collisionality regimes. The investigation of the corresponding behavior of the impurity density and the identification of conditions for favorable coupling between the two are in progress and will be addressed in future work.

## 1. Introduction: recent developments in impurity transport

The transport of impurities in three dimensional toroidal magnetic fields has received much attention from the stellarator community. The accumulation of impurities in the center of the confinement region has been observed to often limit the discharge duration and is considered to be a potential handicap for the development of stellarator reactors. In the framework of neoclassical theory, this accumulation has been generally ascribed to the inward convection caused by the radial electric field acting on the high-$Z$ ions in the absence of a so-called temperature screening effect in non-axisymmetric systems†. In a qualitative sense, these expectations are consistent with the general trend observed in the impurity confinement time [Burhenn et al., 2009].

On a quantitative level, the question of whether or not the observed impurity fluxes agree with the neoclassical estimations based on the solution of approximate

† Recently, both the prevalence of the radial electric field in the transport of impurities [Helander et al., 2017] and the absence of impurity screening in three dimensional magnetic fields [Velasco et al., 2017, Helander et al., 2017] has been brought into question for some relevant collisionality regimes.

versions of the drift kinetic equation is more difficult to answer, for these comparisons are often fragmented, dealing with a reduced number of plasma profiles and based on different measuring techniques. The fundamental output of the neoclassical modeling of impurities is the spatially resolved radial particle flux of a charge state of a certain impurity species, frequently denoted by $\Gamma_z$, and it is often the case that this very quantity is not experimentally accessible, which complicates the direct quantitative comparisons. The experimental determination of impurity fluxes is nevertheless possible from the measurements of absolute density‡ of three consecutive charge states of the impurity species [Langenberg et al., 2017] with X-ray or VUV spectrometers, which allows to estimate the source term of the central charge state. Charge exchange spectroscopy provides measurements of the density of fully striped medium-low-$Z$ impurities like $C^{6+}$. In as much as the plasma conditions (namely, the electron density and temperature) allow to assert that only the fully striped species is present in significant numbers, these measurements provide a zero-flux density profile in stationary conditions or allow to compute fluxes from the evolution of the profiles [Ida et al., 2009].

The kinetic modeling of impurity dynamics and transport has undergone recent improvements with the inclusion of terms usually considered of secondary importance for the calculation of, e.g., ion or electron heat fluxes, but whose charge dependence make them relevant for impurity dynamics [García-Regaña et al., 2013]. These terms relate to the modification of the trajectories of highly charged ion species in a spatially varying electrostatic potential field. As a matter of fact, this has brought up the relevance of the measurement of the electrostatic potential variations along the flux surfaces [Pedrosa et al., 2015], often termed $\varphi_1$, and the benchmarking of its numerical computation [García-Regaña et al., 2017]. These extended neoclassical models have started to be used to revisit some of the previous calculations of neoclassical fluxes and have shown substantial deviations for some machines and plasma conditions [García-Regaña et al., 2017].

In Calvo et al. [2017] the ion heat flux in the low-collisionality regimes below the so-called $1/\nu$-regime have been revisited with a self consistent treatment of the electrostatic potential variations in the drift kinetic and the quasi-neutrality equations. In this contribution we summarise previous results on the size of $\varphi_1$ in several low collisionality regimes and discuss its parity under stellarator-symmetry transformations. This will be shown to determine the corresponding parity of the impurity density variations that will effectively couple to the former to produce a net radial transport through the $E \times B$ associated to $\varphi_1$. In section 2 we introduce the mechanism of radial $E \times B$ impurity transport, discuss some of its properties and motivate the analysis of the partiy of $\varphi_1$ under stellarator-symmetry transformation. This analysis is presented in section 3 for the so-called $1/\nu$, $\sqrt{\nu}$ and plateu regimes. Section 3 does not fully answer the question of the title of this contribution: there remain to be studied the size and parity of the variations of the impurity density along flux surfaces for the relevant collisionality regimes. This will be addressed in future work to complete the analysis of the expected size of the transport driven by the $E \times B$ advection of the variations impurity density along the flux surfaces.

‡ The determination of the absolute number density of a impurity requires an absolute calibration. When only a relative calibration is available, the flux divided by the density $\Gamma_z/n_z$, with units of velocity, can be estimated, which also lends itself to a direct comparison with simulations.

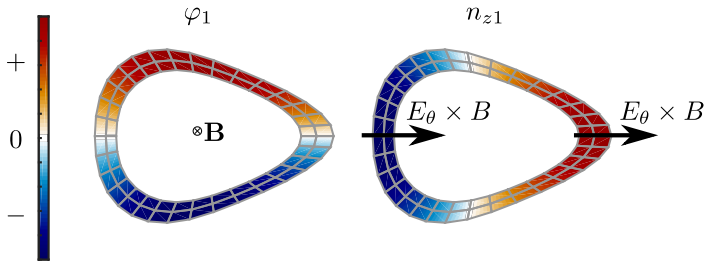


**Figure 1.** Illustration of the radial flux caused by the coupling of electrostatic potential and impurity density variations.

## 2. How tangential electric fields can cause radial transport of impurities

In hot magnetically confined plasmas, the electrostatic potential $\varphi(\mathbf{x})$ is approximately constant along the field lines, just like the distribution functions of the plasma particles are kept approximately a constant Maxwellian along them by the fast parallel streaming of particles. The corrections to the distribution functions that are responsible for the transport of particles and energy across the field lines do display parallel variations. For the size of these for ions and electrons would be different by a factor $\sqrt{m_i/m_e}$ (with $m_i$ and $m_e$ the ion and electron masses respectively), were $\varphi$ perfectly constant along the flux surface, a parallel variation in this function is needed to keep local charge neutrality. This variation will produce a local $E \times B$ drift with a radial component. If impurity plasma particles are found in somewhat greater number in the regions where the radial component of this drift is outward directed, on a flux-surface-average sense, impurities will drift out due to the variations of $\varphi$. This is illustrated in figure 1.

### *2.1. Spatial coordinates*

To make this heuristic description somewhat more rigorous, we will introduce the magnetic coordinates and geometric definitions. Let

$$\mathbf{B} = \Psi_t'(r)\nabla r \times \nabla(\theta - \iota(r)\zeta) \tag{2.1}$$

be the magnetic field, where $r$ is a radial coordinate labeling magnetic surfaces, $\theta$ and $\zeta$ are, respectively, poloidal and toroidal Boozer angles parameterizing the surface, $\iota(r)$ is the rotational transform, $\Psi_t(r)$ is the toroidal magnetic flux over $2\pi$, and a prime indicates a derivative with respect to $r$. In covariant coordinates, $\mathbf{B}$ takes the form

$$\mathbf{B} = \beta\nabla r + I_t(r)\nabla\theta + I_p(r)\nabla\zeta. \tag{2.2}$$

In Boozer coordinates, the volume element $\mathcal{J} := (\nabla r \cdot (\nabla\theta \times \nabla\zeta))^{-1}$ is conveniently written in terms of $B$, the magnitude of the magnetic field $\mathbf{B}$,

$$\mathcal{J} = \frac{V'(r)}{4\pi^2}\frac{\langle B^2\rangle}{B^2}, \tag{2.3}$$

where $\langle(\cdot)\rangle_r$ stands for the flux-surface average

$$\langle(\cdot)\rangle = V'(r)^{-1}\int_0^{2\pi} \mathrm{d}\theta \int_0^{2\pi} \mathrm{d}\zeta\, \mathcal{J}(\cdot) \tag{2.4}$$

and

$$V'(r) = \int_0^{2\pi} \mathrm{d}\theta \int_0^{2\pi} \mathrm{d}\zeta \, \mathcal{J} \tag{2.5}$$

is the radial derivative of the volume $V(r)$ enclosed by the flux surface labeled by $r$.

In low collisionality regimes (see subsections 3.3 and 3.4), the expressions resulting from a drift-kinetic calculation are often written in terms of coordinates adapted to the magnetic field lines, $\alpha$ and $l$. The coordinate $\alpha \in [-\pi, \pi]$ is an angle that labels field lines on the surface. For us, it will be defined by the curve $\zeta = 0$. We take $\alpha = 0$ at $\theta = \pi(1 - \iota)$ because the stellarator-symmetry transformation will take a simple form with this choice (see subsection 3.1). Once a value of $\alpha$ has been fixed, the coordinate $l$, the arc length of the magnetic field line, locates a point along the line labeled by $\alpha$. For each $\alpha$, the value $l = 0$ is defined by the curve $\zeta = 0$. The maximum value of $l$ for each $\alpha$, denoted by $L_\alpha$, is determined following the line until it hits the curve $\zeta = 0$ again.

In these coordinates the magnetic field reads

$$\mathbf{B} = \Psi_t'(r) \nabla r \times \nabla \alpha \tag{2.6}$$

and the expression for the flux-surface average is recast into

$$\langle (\cdot) \rangle = V'(r)^{-1} \int_{-\pi}^{\pi} \mathrm{d}\alpha \int_0^{L_\alpha} \mathrm{d}l \, \Psi_t' B^{-1} (\cdot), \tag{2.7}$$

with

$$V'(r) = \int_{-\pi}^{\pi} \mathrm{d}\alpha \int_0^{L_\alpha} \mathrm{d}l \, \Psi_t' B^{-1}. \tag{2.8}$$

We will be often using $(\alpha, l)$ coordinates in section 3.

### *2.2. Radial impurity flux and the expected size of the radial $E \times B$ advection*

An expression for the radial flux of a plasma species $z$ of charge $q_z = Z_z e$ ($e$ is the proton charge) can be obtained from its momentum balance equation

$$\nabla \cdot \mathbf{\Pi}_z = Z_z e n_z \left( -\nabla \varphi + \mathbf{u}_z \times \mathbf{B} \right) + \mathbf{R}_z \ , \tag{2.9}$$

dotted with the covariant poloidal basis vector, $\mathbf{e}_\theta = \partial_\theta \mathbf{x}$, of a magnetic coordiante system like the Boozer coordinates introduced before, and flux-surface averaged

$$\langle \Gamma_z \cdot \nabla \Psi_t \rangle = - \langle n_z \mathbf{e}_\theta \cdot \nabla \varphi \rangle + \frac{1}{Z_z e} \left( \langle \mathbf{e}_\theta \cdot \mathbf{R}_z \rangle - \langle \mathbf{e}_\theta \cdot \nabla \cdot \mathbf{\Pi}_z \rangle \right). \tag{2.10}$$

In these expression $\Gamma_z = n_z \mathbf{u}_z$ is the particle flux, $n_z$ is the particle number density, $\mathbf{u}_z$ is the fluid velocity, $\mathbf{\Pi}_z$ is the pressure tensor, the collisional friction of the species $z$ with all other plasmas species is $\mathbf{R}_z = \sum_s \mathbf{R}_{zs}$ and $\varphi(\mathbf{x})$ is the electrostatic potential.

For the interpretation of the transport terms it is convenient to add to equation (2.10) the projection of (2.9) on a vector $u\mathbf{B}$ defined such that $\nabla \cdot (\mathbf{e}_\theta + u\mathbf{B}) = 0$.

Then, defining $\boldsymbol{h} = \mathbf{e}_\theta + u\mathbf{B}$ one gets to the more familiar form†

$$\langle \Gamma_z \cdot \nabla \Psi_t \rangle = -\langle n_z \boldsymbol{h} \cdot \nabla \varphi \rangle + \frac{1}{Z_z e}\left( \langle \boldsymbol{h} \cdot \mathbf{R}_z \rangle + \left\langle (p_{z\parallel} - p_{z\perp}) \boldsymbol{h} \cdot \frac{\nabla B}{B} \right\rangle \right), \quad (2.11)$$

where $p_{z\parallel}$ and $p_{z\perp}$ are the parallel and perpendicular components of the traceless part of the gyrotropic pressure tensor. The first term of the RHS of (2.11) is the radial $E \times B$ advection of impurity density that we described heuristically before. If we split both the electrostatic potential and density in a part constant on flux surfaces plus a smaller correction,

$$\varphi = \varphi_0(r) + \varphi_1 + \ldots, \qquad n_z = n_{z0}(r) + n_{z1} + \ldots\ , \quad (2.12)$$

we see that this term involves only the non-constant parts of the impurity density $n_{z1}$ and electrostatic potential $\varphi_1$, for $\boldsymbol{h} \cdot \nabla \varphi_0 = 0$ and $\langle \boldsymbol{h} \cdot \nabla \varphi_1 \rangle = 0$. That is, the lowest-order non-zero contribution from the first term in the RHS of (2.11) is $-\langle n_{z1} \boldsymbol{h} \cdot \nabla \varphi_1 \rangle$.Therefore, the amplitude and the relative phase of the variations $\varphi_1$ and $n_{z1}$ will determine the size and direction of the radial flux produced by this term. A situation in which impurities would be transported outwards is depicted in figure 1.

We note that expression (2.11) is valid also for main ions but, nevertheless, the first term in equation (2.11) does not cause main ion transport. This is due to the fact that, in a plasma of low impurity content with similar electron and ion temperatures like those of relevance of nuclear fusion, $\varphi_1$ is determined by the variations of the main ion density as $\varphi_1 = (T_e/Z_i e)(n_{i1}/n_{i0})$, where sub-indices $e$ and $i$ denote electrons and main ions respectively and $T_e$ is the electron temperature. This follows from the quasineutrality condition with the electron density variation given to leading order by its adiabatic response.‡

For the purpose of interpreting experimental observations it is useful to know about the expected charge $Z_z$ and mass $m_z$ dependence of a transport term and whether it would contribute to the diffusion $D$ or convection $V$ in the usual split $\Gamma_z = -D(d\langle n_z \rangle / dr) + V \langle n_z \rangle$. In the case of the $\langle n_{z1} \boldsymbol{h} \cdot \nabla \varphi_1 \rangle$ term, for a given $\varphi_1$ determined by the ion drift-kinetics, the dependencies are implicit in the size and phase of the impurity density variations, $n_{z1}$ and will in general depend on the collisionality regime and the size of the $E \times B$ poloidal drift relative the impurity thermal velocity. As an illustration of a particular situation, in Alonso et al. [2016] a fluid model of $n_{z1}$ showed relatively small dependencies on $Z_z$ and $m_z$ due to a partial compensation of the inertia and friction terms for the collisional, medium$-Z$ impurities characteristic of the plasma conditions of the neutral-beam-heated plasmas in the TJ-II stellarator. In that same reference, $n_{z1}$ was mainly dependent on the radial electric field and main ion pressure gradient and its radial $E \times B$ transport would therefore account as convection. This is due to the fact that, in

† In fact $\boldsymbol{h}$ is closely related to the poloidal covariant basis vector of a magnetic coordinate system with constant Jacobian known as the Hamada coordinates (see e.g. Sugama and Nishimura [2002, Appendix A]). We note here that, as it is easy to show, the funcion $u(r, \theta, \phi)$ is stellarator symmetric in the sense defined in section 3.

‡ At this point it is interesting to note that the two regimes of 'anomalous' expulsion of impurities known as the high-density $H$-mode [McCormick et al., 2002] and impurity hole [Yoshinuma et al., 2009] regimes, display remarkably steep gradients in the main ion profiles associated with transport barriers. In the interperation of those conditions, turbulence is often put forward as the cause of the degradation of the impurity confinement without an articulation of how is that turbulence species-selective.

the fluid modeling, the dependency on the impurity radial density gradient enters through the impurity diamagnetic velocity, which is usually smaller than the ion diamagnetic and the poloidal $E \times B$ velocities [Alonso et al., 2016].

To actually affect the radial transport of a impurity species through the term under discussion here, it has to be able to compete with the radial fluxes caused by the friction with other species and the viscosity (second and third terms respectively in the RHS of equation (2.11)). Defining the normalised gyroradius of a species $s$ as $\rho_{s*} = v_{ts}/\Omega_s R_0$ with the termal velocity $v_{ts} = \sqrt{T_s/m_s}$ , the gyrofrequency $\Omega_s = Z_s eB/m_s$ and $R_0$ the major radius of the device, the flux caused by the $\langle n_{z1}\boldsymbol{h}\cdot\nabla\varphi_1\rangle$ term is of order

$$\frac{1}{\Psi_t' n_{z0}}\langle n_{z1}\boldsymbol{h}\cdot\nabla\varphi_1\rangle \sim \left(\frac{Z_z}{Z_i}\frac{R_0}{r}\rho_{i*}\right)\rho_{z*}^2 v_{tz} \ , \tag{2.13}$$

where $T_e \sim T_z$ has been assumed; that is, roughly smaller than the other two terms in the RHS of equation (2.11) by a normalised ion gyroradius factor. While this fact would appear to make it difficult for this term to compete with friction and/or viscosity, the stellarator-specific low-collisionality regimes [see e.g. Calvo et al., 2017] in conjunction with impurity-specific parallel dynamics [see e.g. Braun and Helander, 2010], can bring up the size of the density variations considerably above their nominal size (2.13).

As a first step to assess if and when this term can become competitive in the next section we will discuss the expected size of $\varphi_1$ in asymptotic low-collisionality regimes. Furthermore, we will show that the leading order $\varphi_1$ in those regimes has a definite parity with respect to the stellarator symmetry transformation $(\theta,\phi) \mapsto (-\theta,-\phi)$. This is of relevance for the question at hand, for according to equation (2.11), for a given parity of $\varphi_1$, only variations of impurity density $n_{z1}$ with opposite parity will effectively couple to them to give a net radial transport. The sign or direction of this flux depend on the relative phase phase between the two being $+\pi/2$ (as in figure 1) or $-\pi/2$. Advancing results from the next section, it is interesting to note that the sign of $\varphi_1$ will depend on specific relations of the thermodynamic forces, which, in principle, would allow to revert the flux direction by profile shaping. This is of course somewhat constrained by the relationship of the thermodynamic forces introduced by the ambipolarity condition.

## 3. Parity of $\varphi_1$ under stellarator-symmetry transformations

In this section we introduce the stellarator-symmetry transformation and compile results on the size and parity of $\varphi_1$ for the $1/\nu$, $\sqrt{\nu}$ and plateu collisionality regimes. The results of this section are summarized in figure 2.

### *3.1. Stellarator-symmetry transformation*

Given a magnetic surface $r$ and Boozer angles $\theta$ and $\zeta$, we define the stellarator-symmetry transformation $\mathfrak{s}$, acting on points on the surface, by

$$\mathfrak{s}(\theta,\zeta) = (-\theta,-\zeta). \tag{3.1}$$

Taking $(\theta,\zeta) \in [0,2\pi]\times[0,2\pi]$, it is easy to realize that $\mathfrak{s}$ can be viewed as a reflection across the point $(\theta,\zeta) = (\pi,\pi)$.

Stellarator magnetic fields are designed such that $B(\theta,\zeta)$ (we frequently omit

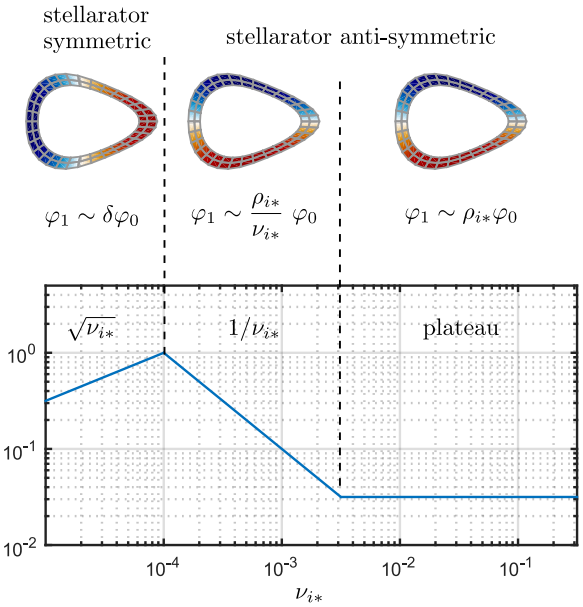


**Figure 2.** Summary of the parity and size of $\varphi_1$ in the low-collisionality regimes in a diffusivity versus collsionality plot. The parameter $\delta$ is the size of the deviation of the magnetic field strength from omnigeneity (see section 3.4).

the dependence on $r$) is stellarator symmetric (sometimes we will simply say "symmetric"); that is, such that $\mathfrak{s}^* B = B$, where the pullback of $B$ by $\mathfrak{s}$ is defined as

$$\mathfrak{s}^* B(\theta, \zeta) = B(\mathfrak{s}(\theta, \zeta)). \tag{3.2}$$

Throughout this section we assume that $B$ is symmetric.

The transformation $\mathfrak{s}$ in coordinates $\alpha$ and $l$ (we do not change its name; no confusion is expected) becomes

$$\mathfrak{s}(\alpha, l) = (-\alpha, L_\alpha - l). \tag{3.3}$$

Note that if $B$ is symmetric, then $L_\alpha = L_{-\alpha}$. Analogously, if $l_{b_1}(\alpha)$ and $l_{b_2}(\alpha)$ are the left and right bounce points of a trapped trajectory, then $\mathfrak{s}(\alpha, l_{b_1}(\alpha)) = (-\alpha, l_{b_2}(-\alpha))$ and $\mathfrak{s}(\alpha, l_{b_2}(\alpha)) = (-\alpha, l_{b_1}(-\alpha))$.

Equipped with the notation above, it is straightforward to prove the following result. Let

$$F(\alpha, v, \lambda, \sigma) = \int_{l_{b_1}(\alpha)}^{l_{b_2}(\alpha)} K(B(\alpha, l), v, \lambda) f(\alpha, l, v, \lambda, \sigma) \mathrm{d}l \tag{3.4}$$

be a function defined for trapped trajectories. Then,

$$\mathfrak{s}^* F(\alpha, v, \lambda, \sigma) = \int_{l_{b_1}(\alpha)}^{l_{b_2}(\alpha)} K(B(\alpha, l), v, \lambda)\, \mathfrak{s}^* f(\alpha, l, v, \lambda, \sigma) \mathrm{d}l. \tag{3.5}$$

Here, $v$ is the magnitude of the velocity, $\lambda = v_\perp^2/(v^2 B)$ is the pitch-angle coordinate, $v_\perp$ is the component of the velocity perpendicular to $\mathbf{B}$ and $\sigma$ is the sign of the component of the velocity parallel to the magnetic field,

$$v_{||} = \sigma\sqrt{1 - \lambda B}, \tag{3.6}$$

whereas $l_{b_1}$ and $l_{b_2}$ are the bounce points corresponding to the trajectory defined by $\lambda$.

Equation (3.5) says, in particular, that if $f$ is symmetric (resp. antisymmetric), then $F$ is symmetric (resp. antisymmetric).

### *3.2. Quasineutrality equation*

In this section, we assume that the plasma consists of adiabatic electrons and only one species of ions. As said before, we expand the electrostatic potential as

$$\varphi = \varphi_0(r) + \varphi_1 + \dots, \tag{3.7}$$

where $\varphi_0 \sim T_i/Z_i e$. The size of the correction $\varphi_1$ depends on the collisionality regime. We write the piece of the quasineutrality equation determining $\varphi_1$ as

$$\left(\frac{Z_i}{T_i} + \frac{1}{T_e}\right)\varphi_1 = \frac{2\pi}{e n_i}\int_0^\infty \mathrm{d}v \int_0^{B^{-1}} \mathrm{d}\lambda \frac{v^3 B}{|v_{||}|}\frac{1}{2}\left(g_i(\sigma=1) + g_i(\sigma=-1)\right). \tag{3.8}$$

Here, we have used that, for gyrophase-independent functions,

$$\int (\cdot)\mathrm{d}^3 v \equiv \sum_\sigma \int_0^\infty \mathrm{d}v \int_0^{B^{-1}} \mathrm{d}\lambda \frac{\pi B v^3}{|v_{||}|}(\cdot)\mathrm{d}v\mathrm{d}\lambda. \tag{3.9}$$

In equation (3.8) $g_i$ is the dominant piece of the non-adiabatic component of the deviation of the ion distribution function from a Maxwellian distribution. The equation for $g_i$ and its size also depend on the collisionality regime. Finally, we choose $\varphi_1$ such that $\langle\varphi_1\rangle_r = 0$ and $g_i$ such that the right side of (3.8) has vanishing flux-surface average. We have also emphasized that only the component of $g_i$ that is even in the parallel velocity contributes to the right side of (3.8).

### *3.3. Parity of $\varphi_1$ in the $1/\nu$ regime*

Low collisionality regimes are those in which the parallel streaming term is the largest term of the drift-kinetic equation. This implies that $g_i$ does not depend on $l$ and, typically, that $g_i$ in the passing region is negligible compared to $g_i$ in the trapped region. Since $\partial_l g_i = 0$, continuity at the bounce points of trapped trajectories implies that $g_i$ in the trapped region is even in $\sigma$.

In order to find $g_i$ in the trapped region, one has to solve the drift-kinetic equation

$$\sum_\sigma \frac{Z_i e \Psi_t'}{m_i c}\int_{l_{b_1}}^{l_{b_2}} \frac{\mathrm{d}l}{|v_{||}|} C_{ii}^\ell[g_i] = \partial_\alpha J_B \Upsilon_i f_{Mi}, \tag{3.10}$$

where $m_i$ is the ion mass, $c$ is the speed of light,

$$J_B = 2\int_{l_{b_1}}^{l_{b_2}} |v_{||}|\mathrm{d}l \tag{3.11}$$

is the second adiabatic invariant,

$$f_{Mi}(r,v) = n_i(r)\left(\frac{m_i}{2\pi T_i(r)}\right)^{3/2}\exp\left(-\frac{m_i v^2}{2T_i(r)}\right) \tag{3.12}$$

is a Maxwellian distribution,

$$\Upsilon_i = \frac{n_i'}{n_i} + \frac{T_i'}{T_i}\left(\frac{m_i v^2}{2T_i} - \frac{3}{2}\right) + \frac{Z_i e \varphi_0'}{T_i} \tag{3.13}$$

and $C_{ii}^{\ell}$ is the linearized collision operator written in coordinates $v$ and $\lambda$, whose explicit expression is not needed here. We simply point out that it depends on $\alpha$ and $l$ only through $B$ evaluated at $\alpha$ and $l$. Therefore, we can apply the result (3.5) to deduce that the left side of (3.10) conserves the parity of $g_i$. Again, due to (3.5), $J_B$ is symmetric and therefore $\partial_\alpha J_B$ is antisymmetric. Hence, $g_i$ is antisymmetric† under $\mathfrak{s}$.

From (3.10), it is clear that $g_i$ has a size

$$g_i \sim \frac{\rho_{i*}}{\nu_{i*}} f_{Mi}. \tag{3.14}$$

where $\nu_{i*} = \nu_{ii} R_0/v_{ti}$ is the ion collisionality and $\nu_{ii}$ is the ion-ion collision frequency.

The quasineutrality equation (recall (3.8)) reads

$$\left(\frac{Z_i}{T_i} + \frac{1}{T_e}\right)\varphi_1 = \frac{2\pi}{e n_i}\int_0^\infty \mathrm{d}v \int_{B_{\max}^{-1}}^{B^{-1}} \mathrm{d}\lambda \frac{v^3 B}{|v_{||}|} g_i, \tag{3.15}$$

where $B_{\max}$ is the maximum value of $B$ on the magnetic surface. In order to write (3.15), we have used that $g_i$ is even in $\sigma$ and that $g_i$ in the passing region is negligible. Now, it is obvious that in the $1/\nu$ regime

$$\varphi_1 \sim \frac{\rho_{i*}}{\nu_{i*}}\varphi_0. \tag{3.16}$$

Finally, recalling that $g_i$ is stellarator antisymmetric, equation (3.15) implies that $\varphi_1$ is antisymmetric as well.

### *3.4. Parity of $\varphi_1$ in the $\sqrt{\nu}$ regime*

In Calvo et al. [2017] it has been shown that the rigorous derivation of the $\sqrt{\nu}$ regime requires some assumptions on the magnetic configurations. For example, it can be obtained if the stellarator is close to omnigeneity; that is, if $B$ can be written as

$$B = B_0 + B_1, \tag{3.17}$$

where $B_0$ is omnigeneous and $|B_1| \ll |B_0|$. If the stellarator has large aspect ratio, the $\sqrt{\nu}$ regime can also be obtained, even if it is not close to omnigeneity. Here, we assume that the stellarator is close to omnigeneity and that the expansion in $\delta \sim |B_1|/|B_0| \ll 1$ has been carried out. We do not repeat the details of the derivations, but refer the reader to [Calvo et al., 2017]. We also assume that both, $B_0$ and $B_1$ are stellarator symmetric.

In the $\sqrt{\nu}$ regime, the sizes of $g_i$ and $\varphi_1$ are

$$g_i \sim \delta f_{Mi} \tag{3.18}$$

and

$$\varphi_1 \sim \delta\varphi_0. \tag{3.19}$$

Of course, the $\sqrt{\nu}$ regime is a low-collisionality regime and therefore $\partial_l g_i = 0$, $g_i$ in the passing region is negligible for our interests and $g_i$ in the trapped region is even in $\sigma$.

† Equation (3.10), in principle, allows a non-zero stellarator-symmetric component for $g_i$ that is a Maxwellian constant on flux surfaces. However, this Maxwellian has to be zero due to the condition that we chose to impose on $g_i$, explained after (3.9).

After expanding in $\delta$, the quasineutrality equation reads

$$\left(\frac{Z_i}{T_i}+\frac{1}{T_e}\right)\varphi_1=\frac{2\pi}{en_i}\int_0^\infty \mathrm{d}v\int_{B_{0,\max}^{-1}}^{B^{-1}}\mathrm{d}\lambda\frac{v^3B_0}{|v_{||}^{(0)}|}g_i, \tag{3.20}$$

where a superindex (0) indicates that the corresponding quantity has been written including only $B_0$ (instead of $B$). For example,

$$v_{||}^{(0)}=\sigma v\sqrt{1-\lambda B_0}\,. \tag{3.21}$$

The drift-kinetic equation for $g_i$ in the $\sqrt{\nu}$ regime† incorporates the effect of the tangential drifts. Namely,

$$-\partial_r J^{(0)}\partial_\alpha g_i+\partial_\alpha J^{(1)}\Upsilon_i f_{Mi}=\sum_\sigma\frac{Z_i e\Psi_t'}{m_i c}\int_{l_{b_{10}}}^{l_{b_{20}}}\frac{\mathrm{d}l}{|v_{||}^{(0)}|}C_{ii}^{\ell(0)}[g_i], \tag{3.22}$$

where

$$\partial_r J^{(0)}=-\int_{l_{b_{10}}}^{l_{b_{20}}}\frac{\lambda v\partial_r B_0+2Z_i e/(m_i v)\varphi_0'}{\sqrt{1-\lambda B_0}}\mathrm{d}l \tag{3.23}$$

is a flux function and

$$J^{(1)}=-\int_{l_{b_{10}}}^{l_{b_{20}}}\frac{\lambda vB_1+2Z_i e/(m_i v)\varphi_1}{\sqrt{1-\lambda B_0}}\mathrm{d}l. \tag{3.24}$$

The largest piece of $g_i$ is found by dropping the collision term in (3.22), giving

$$g_i=\frac{\widetilde{J}^{(1)}}{\partial_r J^{(0)}}\Upsilon_i f_{Mi} \tag{3.25}$$

with

$$\widetilde{J}^{(1)}=J^{(1)}-\frac{1}{2\pi}\int_0^{2\pi}J^{(1)}\mathrm{d}\alpha, \tag{3.26}$$

where we have chosen $\int_0^{2\pi} g_i\,\mathrm{d}\alpha=0$ (it is easy to check that this condition implies that the right side of (3.20) vanishes). Although (3.25) gives no contribution to the radial neoclassical fluxes, it provides the dominant contribution to the quasineutrality equation (3.20).

Inserting (3.25) in (3.20) and rearranging a bit, we find

$$\begin{aligned}\left(\frac{Z_i}{T_i}+\frac{1}{T_e}\right)\varphi_1-\frac{2\pi}{en_i}\int_0^\infty \mathrm{d}v\int_{B_{0,\max}^{-1}}^{B^{-1}}\mathrm{d}\lambda\frac{v^3B_0}{|v_{||}^{(0)}|}\frac{\Upsilon_i f_{Mi}}{\partial_r J^{(0)}}\widetilde{J}_\varphi^{(1)}\\ =\frac{2\pi}{en_i}\int_0^\infty \mathrm{d}v\int_{B_{0,\max}^{-1}}^{B^{-1}}\mathrm{d}\lambda\frac{v^3B_0}{|v_{||}^{(0)}|}\frac{\Upsilon_i f_{Mi}}{\partial_r J^{(0)}}\widetilde{J}_B^{(1)},\end{aligned} \tag{3.27}$$

where

$$J_B^{(1)}=-\lambda v\int_{l_{b_{10}}}^{l_{b_{20}}}\frac{B_1}{\sqrt{1-\lambda B_0}}\mathrm{d}l, \tag{3.28}$$

† In order to truly be in the $\sqrt{\nu}$ regime, we need not only to have sufficiently small $\nu_{i*}$. It is also required that $\partial_r J^{(0)}$ never vanish or that it vanish for $v\gg v_{ti}$, as explained in [Calvo et al., 2017].

$$J_\varphi^{(1)} = -\frac{2Z_i e}{m_i v}\int_{l_{b_{10}}}^{l_{b_{20}}} \frac{\varphi_1}{\sqrt{1-\lambda B_0}}\mathrm{d}l, \tag{3.29}$$

$$\widetilde{J}_B^{(1)} = J_B^{(1)} - \frac{1}{2\pi}\int_0^{2\pi} J_B^{(1)}\mathrm{d}\alpha \tag{3.30}$$

and

$$\widetilde{J}_\varphi^{(1)} = J_\varphi^{(1)} - \frac{1}{2\pi}\int_0^{2\pi} J_\varphi^{(1)}\mathrm{d}\alpha. \tag{3.31}$$

Invoking (3.5), we straightforwardly realize that the term on the right side of (3.27) is symmetric and that the operator acting on $\varphi_1$ on the left side conserves parity under $\mathfrak{s}$. Hence, $\varphi_1$ is stellarator symmetric.

### *3.5. Parity of $\varphi_1$ in the plateau regime*

In the plateau regime, we can derive an analytical expression for $\varphi_1$, and we do it in detail in this section.

The relevant drift-kinetic equation in this case is

$$v_{||}\hat{\mathbf{b}}\cdot\nabla g_i + \Upsilon_i \mathbf{v}_M\cdot\nabla r f_{Mi} = C_{ii}^\ell[g_i]. \tag{3.32}$$

Using (2.1), one gets the expression

$$\hat{\mathbf{b}}\cdot\nabla = \frac{\Psi_t'}{B}\frac{1}{\mathcal{J}}(\partial_\zeta + \iota\partial_\theta) \tag{3.33}$$

for the parallel streaming operator.

Employing that $\theta$ and $\zeta$ are Boozer coordinates, we can write the radial magnetic drift as

$$\mathbf{v}_M\cdot\nabla r = \frac{v^2}{\Omega_i B^2}\left(\frac{\lambda B}{2}-1\right)\frac{1}{\mathcal{J}}\left(I_p\partial_\theta B - I_t\partial_\zeta B\right). \tag{3.34}$$

The plateau regime is a collisionality regime in which radial transport (and also $\varphi_1$) is determined by a small layer in phase space around $v_{||}=0$. As a consequence, the pitch-angle piece of the collision operator dominates,

$$C_{ii}^\ell[g_i] \approx \frac{\nu_\lambda v_{||}}{v^2 B}\partial_\lambda\left(v_{||}\lambda\partial_\lambda g_i\right), \tag{3.35}$$

where $\nu_\lambda(v)$ is defined in [Calvo et al., 2017].

Typically, the solution of the plateau regime is obtained using the coordinate $\xi = v_{||}/v$, in which the form of the assumptions and the calculation itself are simpler. Denote by $\bar{g}_i$ the function $g_i$ expressed in coordinates $v$ and $\xi$. Then,

$$v_{||}\hat{\mathbf{b}}\cdot\nabla g_i = \xi v\hat{\mathbf{b}}\cdot\nabla\bar{g}_i - \frac{v}{2B}\hat{\mathbf{b}}\cdot\nabla B(1-\xi^2)\partial_\xi\bar{g}_i \tag{3.36}$$

and

$$C_{ii}^\ell[\bar{g}_i] \approx \frac{\nu_\lambda}{4}\partial_\xi\left[(1-\xi^2)\partial_\xi\bar{g}_i\right]. \tag{3.37}$$

In coordinates $v$ and $\xi$, the radial magnetic drift reads

$$\mathbf{v}_M\cdot\nabla r = -\frac{v^2}{2\Omega_i B^2}\left(1+\xi^2\right)\frac{1}{\mathcal{J}}\left(I_p\partial_\theta B - I_t\partial_\zeta B\right). \tag{3.38}$$

The plateau regime only exists if the inverse aspect ratio, $\epsilon = r/R_0$, is small. If this is the case, one can write

$$B(r,\theta,\zeta) = B_{00} + \tilde{B}(r,\theta,\zeta), \tag{3.39}$$

where $B_{00}$ is constant and $\tilde{B} \sim \epsilon B_{00}$. From (2.3), it is clear that

$$\mathcal{J} = \mathcal{J}_1 + O(\epsilon^2 R_0^2), \tag{3.40}$$

where $\mathcal{J}_1 \sim \epsilon R_0^2$. Hence, the right side of (3.38) does not scale with $\epsilon$.

A large, localized distribution function around $\xi = 0$ can happen when the first term on the right side of (3.36) balances the right side of (3.37), whereas at the same time the first term on the right side of (3.36) is much larger than the second term on the right side of (3.36). This happens when† $\nu_{i*} \ll 1$ and

$$\frac{\epsilon^{3/2}}{\nu_{i*}} \ll 1. \tag{3.41}$$

Then, the size of the layer is

$$\delta\xi \sim \nu_{i*}^{1/3}. \tag{3.42}$$

Finally (from now on, we drop the bar from $\bar{g}_i$), the equation to be solved in order to find the dominant piece of $g_i$ is

$$\frac{\Psi_t'}{B_{00}\mathcal{J}_1}\xi v(\partial_\zeta + \iota\partial_\theta)g_i - \frac{\nu_\lambda}{4}\partial_\xi^2 g_i = -\Upsilon_i \mathbf{v}_M \cdot \nabla r\Big|_{\substack{\xi=0\\ \epsilon=0}} f_{Mi}, \tag{3.43}$$

with

$$\mathbf{v}_M \cdot \nabla r\Big|_{\substack{\xi=0\\ \epsilon=0}} = -\frac{v^2}{2(\Omega_i)_{00}B_{00}^2}\frac{1}{\mathcal{J}_1}\left(I_p\partial_\theta\tilde{B} - I_t\partial_\zeta\tilde{B}\right) \tag{3.44}$$

and $(\Omega_i)_{00} = Z_i e B_{00}/(m_i c)$.

We solve (3.43) in Fourier space. We denote

$$\tilde{B} = \sum_{m,n}\tilde{B}_{mn}e^{i(m\theta+n\zeta)}, \tag{3.45}$$

$$g_i = \sum_{m,n} g_{mn}e^{i(m\theta+n\zeta)}, \tag{3.46}$$

and so on. Thus, (3.43) becomes

$$\frac{4\Psi_t' R_0}{B_{00}\mathcal{J}_1}\xi i(n+\iota m)g_{mn} - \nu_{\lambda *}\partial_\xi^2 g_{mn} = -\frac{4R_0}{v}\Upsilon_i\left(\mathbf{v}_M\cdot\nabla r\Big|_{\substack{\xi=0\\ \epsilon=0}}\right)_{mn} f_{Mi}, \tag{3.47}$$

where $\nu_{\lambda *} := \nu_\lambda R_0/v$ and

$$\left(\mathbf{v}_M\cdot\nabla r\Big|_{\substack{\xi=0\\ \epsilon=0}}\right)_{mn} = -\frac{v^2}{2(\Omega_i)_{00}B_{00}^2}\frac{1}{\mathcal{J}_1} i\left(I_p m - I_t n\right)\tilde{B}_{mn}. \tag{3.48}$$

Note that, since $\tilde{B}$ is stellarator symmetric (and, of course, real), $\tilde{B}_{mn}$ is real and $\tilde{B}_{-m,-n} = \tilde{B}_{mn}$. Then,

$$\left(\mathbf{v}_M\cdot\nabla r\Big|_{\substack{\xi=0\\ \epsilon=0}}\right)_{-m,-n} = -\left(\mathbf{v}_M\cdot\nabla r\Big|_{\substack{\xi=0\\ \epsilon=0}}\right)_{mn} \tag{3.49}$$

and, obviously, the coefficients

$$\left(\mathbf{v}_M\cdot\nabla r\Big|_{\substack{\xi=0\\ \epsilon=0}}\right)_{mn} \tag{3.50}$$

are imaginary.

† Note that $\nu_{i*} \sim \nu_\lambda(v_t)R_0/v_{ti}$.

It is convenient to employ the rescaled coordinate

$$\xi = \nu_{\lambda *}^{1/3} A \eta, \tag{3.51}$$

with

$$A = \left( \frac{B_{00} \mathcal{J}_1}{4 R_0 \Psi_t' (n + \iota m)} \right)^{1/3} \tag{3.52}$$

and write (3.47) as (we do not change the notation for $g_i$)

$$i \eta g_{mn} - \partial_\eta^2 g_{mn} = \frac{i S_{mn}}{\nu_{\lambda *}^{1/3} A}, \tag{3.53}$$

where

$$S_{mn} = \frac{1}{2 (\Omega_i)_{00} B_{00} \Psi_t'} \frac{I_p m - I_t n}{n + \iota m} \tilde{B}_{mn} v \Upsilon_i f_{Mi}. \tag{3.54}$$

The solution of (3.53) written in the coordinate $\xi$ is

$$g_{mn} = \frac{i S_{mn}}{\nu_{\lambda *}^{1/3} A} \int_0^\infty e^{-z^3/3} \exp \left( -i \frac{\xi z}{\nu_{\lambda *}^{1/3} A} \right) \mathrm{d}z. \tag{3.55}$$

The expression for $\varphi_1$ is found by using (3.55) in (3.8). Writing the integral on the right side of (3.8) in coordinates $v$ and $\xi$, one gets

$$\left( \frac{Z_i}{T_i} + \frac{1}{T_e} \right) \varphi_1 = \frac{4\pi}{e n_i} \int_0^\infty \mathrm{d}v v^2 \int_0^v \mathrm{d}\xi \, \frac{1}{2} \left( g_i(\sigma = 1) + g_i(\sigma = -1) \right). \tag{3.56}$$

Employing (3.55) and the identity

$$\lim_{k \to 0^+} \frac{1}{k} \int_0^\infty e^{-z^3/3} \cos \left( \frac{1}{k} x z \right) \mathrm{d}z = \pi \delta(x), \tag{3.57}$$

we obtain an explicit solution for the largest piece of $\varphi_1$ in an asymptotic expansion in $\nu_{i*} \ll 1$,

$$\varphi_1 = \frac{i 2 \pi^2}{e n_i} \left( \frac{Z_i}{T_i} + \frac{1}{T_e} \right)^{-1} \frac{\left( \int_0^\infty v^3 \Upsilon_i f_{Mi} \mathrm{d}v \right)}{(\Omega_i)_{00} B_{00} \Psi_t'} \sum_{m,n} \frac{I_p m - I_t n}{|n + \iota m|} \tilde{B}_{mn} \, e^{i(m\theta + n\zeta)} \tag{3.58}$$

In particular, we learn that

$$\varphi_1 \sim \rho_{i*} \varphi_0 \tag{3.59}$$

and that $\varphi_1$ is stellarator antisymmetric.

## References

J A Alonso, J L Velasco, I Calvo, T Estrada, J M Fontdecaba, J M García-Regaña, J Geiger, M Landreman, K J McCarthy, F Medina, B Ph Van Milligen, M A Ochando, F I Parra, the TJ-II Team, and the W7-X Team. Parallel impurity dynamics in the tj-ii stellarator. *Plasma Physics and Controlled Fusion*, 58(7): 074009, jun 2016. URL `http://stacks.iop.org/0741-3335/58/i=7/a=074009`.

S Braun and P Helander. Pfirsch–Schlüter impurity transport in stellarators. *Physics of Plasmas*, 17(7):072514, 2010. . URL `http://dx.doi.org/10.1063/1.3458901`.

R. Burhenn, Y. Feng, K. Ida, H. Maassberg, K.J. McCarthy, D. Kalinina, M. Kobayashi, S. Morita, Y. Nakamura, H. Nozato, S. Okamura, S. Sudo, C. Suzuki, N. Tamura, A. Weller, M. Yoshinuma, and B. Zurro. On impurity handling in high performance stellarator/heliotron plasmas. *Nuclear Fusion*, 49 (6):065005, 2009. URL http://stacks.iop.org/0029-5515/49/i=6/a=065005.

Iván Calvo, Felix I Parra, José Luis Velasco, and J Arturo Alonso. The effect of tangential drifts on neoclassical transport in stellarators close to omnigeneity. *Plasma Physics and Controlled Fusion*, 59(5):055014, 2017. URL http://stacks.iop.org/0741-3335/59/i=5/a=055014.

J.M. García-Regaña, C.D. Beidler, R. Kleiber, P. Helander, A. Mollén, J.A. Alonso, M. Landreman, H. Maaßberg, H.M. Smith, Y. Turkin, and J.L. Velasco. Electrostatic potential variation on the flux surface and its impact on impurity transport. *Nuclear Fusion*, 57(5):056004, 2017. URL http://stacks.iop.org/0029-5515/57/i=5/a=056004.

J M García-Regaña, R Kleiber, C D Beidler, Y Turkin, H Maaßberg, and P Helander. On neoclassical impurity transport in stellarator geometry. *Plasma Physics and Controlled Fusion*, 55(7):074008, 2013. URL http://stacks.iop.org/0741-3335/55/i=7/a=074008.

P. Helander, S. L. Newton, A. Mollén, and H. M. Smith. Impurity transport in a mixed-collisionality stellarator plasma. *Phys. Rev. Lett.*, 118:155002, Apr 2017. . URL https://link.aps.org/doi/10.1103/PhysRevLett.118.155002.

K. Ida, M. Yoshinuma, M. Osakabe, K. Nagaoka, M. Yokoyama, H. Funaba, C. Suzuki, T. Ido, A. Shimizu, I. Murakami, N. Tamura, H. Kasahara, Y. Takeiri, K. Ikeda, K. Tsumori, O. Kaneko, S. Morita, M. Goto, K. Tanaka, K. Narihara, T. Minami, and I. Yamada. Observation of an impurity hole in a plasma with an ion internal transport barrier in the large helical device. *Physics of Plasmas*, 16(5):056111, 2009. . URL http://dx.doi.org/10.1063/1.3111097.

Andreas Langenberg, Novimir Pablant, Oleksandr Marchuk, Daihong Zhang, J Alonso, Rainer Burhenn, Jakob Svensson, Pranay Valson, David Gates, Marc Beurskens, and Robert Wolf. Argon impurity transport studies at wendelstein 7-x using x-ray imaging spectrometer measurements. *Nuclear Fusion*, 2017. URL http://iopscience.iop.org/10.1088/1741-4326/aa70f4.

K. McCormick, P. Grigull, R. Burhenn, R. Brakel, H. Ehmler, Y. Feng, F. Gadelmeier, L. Giannone, D. Hildebrandt, M. Hirsch, R. Jaenicke, J. Kisslinger, T. Klinger, S. Klose, J. P. Knauer, R. König, G. Kühner, H. P. Laqua, D. Naujoks, H. Niedermeyer, E. Pasch, N. Ramasubramanian, N. Rust, F. Sardei, F. Wagner, A. Weller, U. Wenzel, and A. Werner. New advanced operational regime on the w7-as stellarator. *Phys. Rev. Lett.*, 89:015001, Jun 2002. . URL http://link.aps.org/doi/10.1103/PhysRevLett.89.015001.

M.A. Pedrosa, J.A. Alonso, J.M. García-Regaña, C. Hidalgo, J.L. Velasco, I. Calvo, R. Kleiber, C. Silva, and P. Helander. Electrostatic potential variations along flux surfaces in stellarators. *Nuclear Fusion*, 55(5):052001, 2015. URL http://stacks.iop.org/0029-5515/55/i=5/a=052001.

H. Sugama and S. Nishimura. How to calculate the neoclassical viscosity, diffusion, and current coefficients in general toroidal plasmas. *Physics of Plasmas*, 9:4637, 2002.

J.L. Velasco, I. Calvo, S. Satake, A. Alonso, M. Nunami, M. Yokoyama, M. Sato, T. Estrada, J.M. Fontdecaba, M. Liniers, K.J. McCarthy, F. Medina, B. Ph Van Milligen, M. Ochando, F. Parra, H. Sugama, A. Zhezhera, The LHD Experimental

Team, and The TJ-II Team. Moderation of neoclassical impurity accumulation in high temperature plasmas of helical devices. *Nuclear Fusion*, 57(1):016016, 2017. URL http://stacks.iop.org/0029-5515/57/i=1/a=016016.

M. Yoshinuma, K. Ida, M. Yokoyama, M. Osakabe, K. Nagaoka, S. Morita, M. Goto, N. Tamura, C. Suzuki, S. Yoshimura, H. Funaba, Y. Takeiri, K. Ikeda, K. Tsumori, O. Kaneko, and the LHD Experimental Group. Observation of an impurity hole in the large helical device. *Nuclear Fusion*, 49(6):062002, 2009. URL http://stacks.iop.org/0029-5515/49/i=6/a=062002.